

Effect of the range of the potential on two-dimensional melting

Sang Il Lee and Sung Jong Lee

Department of Physics, University of Suwon, Suwon, Kyonggi-Do 445-743, Korea

(Received 26 August 2008; published 27 October 2008)

Insights into the melting of two-dimensional simple atomic systems are presented from investigation of the effect of the range of the interatomic potentials on the existence of hexatic phase, using molecular-dynamics simulations under isobaric-isothermal as well as isochoric-isothermal conditions. We find that longer-ranged interatomic potentials are important for the formation of stable hexatic phases. A schematic plot of the phase diagrams with a hexatic regime is presented capturing the overall shape of the phase boundaries and the behavior of the system. As the range of the potential is varied, the pressure-temperature phase diagram exhibits distinct topologies. For soft longer-ranged Morse potentials, the hexatic phase can coexist with the gaseous phase. On the other hand, as the range gets shorter, the onset point of the hexatic phase, i.e., the lower bound pressure of the hexatic region in the phase diagram, gets shifted upward, and the hexatic phase region no longer touches the gaseous phase.

DOI: [10.1103/PhysRevE.78.041504](https://doi.org/10.1103/PhysRevE.78.041504)

PACS number(s): 64.70.D-, 02.70.Ns, 05.70.Fh, 61.20.Ja

I. INTRODUCTION

Two-dimensional melting [1] has intrigued physicists for many decades. An important milestone was laid by Halperin and Nelson (HN) [2,3] and Young [4], who suggested theoretically (based on the work by Kosterlitz and Thouless [5]) that the two-dimensional melting can occur in two stages of continuous transitions, the first one via the unbinding of dislocations and the second one via the unbinding of disclinations with the intermediate hexatic phase characterized by quasi-long-range orientational order and short-range translational order [6].

A wide variety of experiments were performed on systems including colloids [7–10], liquid crystals [11–14], block copolymers [15], and granular systems [16,17] concerning the possible existence of a hexatic phase and two-stage melting. Also, a lot of efforts were made on computational studies of two-dimensional melting of hard-core potential systems [18–23,26–29] including hard disks or Lennard-Jones potentials [30–32]. Simulation results on these systems tend to favor a first-order transition scenario for melting, although some conflicting results also exist.

In spite of all these efforts, a satisfactory answer has not been obtained yet for one of the most important questions in two-dimensional melting, which is as follows: what condition determines the existence of a hexatic phase and the nature of the melting transition? From these considerations, we are led to investigate the criterion for the existence of the hexatic phase directly in terms of the form of interparticle potential [33,34]. For a given system that is found to support a hexatic phase, one can further ask about the boundary of the region of the stable hexatic phase in the phase diagram.

Our approach to these goals is to investigate through molecular-dynamics (MD) simulations the trend of hexatic phase formations as the range of the potential is varied in simple two-dimensional atomic systems where particles are interacting via the Morse potential,

$$V_M(r) = \epsilon_0 [e^{-\alpha(r-\sigma)} - 1]^2 - \epsilon_0. \quad (1)$$

Here, r is the distance between particles and σ denotes the distance for the minimum of the potential. By setting $\sigma=1$

and $\epsilon_0=1$, we can vary the value of the single parameter α to tune the softness and the range of potential. As can be seen in Fig. 1, larger values of α correspond to shorter-ranged and steeper potentials, while smaller values correspond to longer-ranged and softer potentials.

In actual computation, further adjustment of the potential is made such that the resulting potential has a smooth cutoff at $r_c=2.8\sigma$ by a standard method of vertical shift and linear smoothing. The Morse potential was employed to explain qualitatively different behavior for a wide variety of liquids, varying the softness and the interaction range of the potential [24,25]. Specific examples of the values of α employed to explain different tendencies for the structure of materials include, for example, C_{60} ($\alpha \approx 13.62$), rare gases with Lennard-Jones potential ($\alpha \approx 6$), and alkali metals ($\alpha \approx 3.15$) [24].

We find a thermodynamically stable hexatic phase for the case of a long-ranged (and soft) Morse potential with $\alpha=3.0$. In contrast, in the two cases of modification of the potential where the attractive tail part is replaced by a flat potential, or else where the soft repulsive part is replaced by a very hard repulsive wall, the hexatic phase is strongly suppressed, with the melting proceeding via first-order transitions.

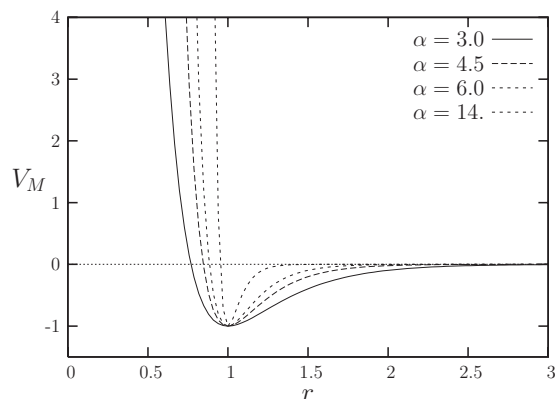


FIG. 1. Morse potential for different values of $\alpha=3.0, 4.5, 6.0$, and 14.

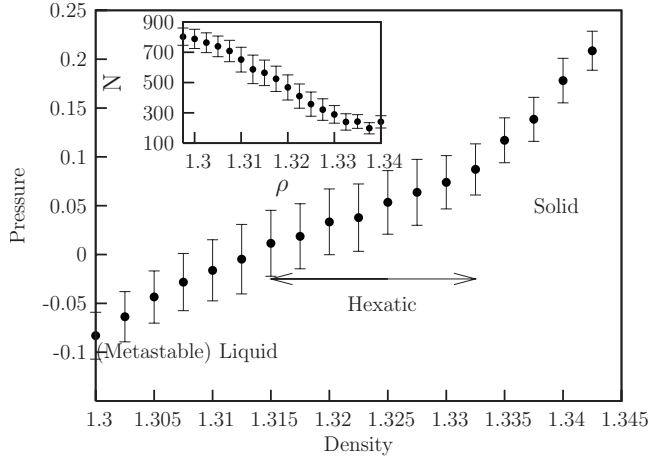


FIG. 2. Pressure vs density for the system with $\alpha=3.0$ at the temperature $T=0.2715$ (which is below the critical point) obtained from NVT ensemble with $N=3600$ particles. The inset shows the number of defects vs density. The solid-hexatic boundary is determined as the point (about $\rho \approx 1.3325$) at which the number of defects increases abruptly (the inset), and the liquid-hexatic boundary is determined from the orientational correlation function in Fig. 3: the decay exponent of the spatial correlation of the orientational correlation has 0.25 near the density $\rho \approx 0.315$.

We also explore the dependence of the topology of the hexatic region as the parameter α is varied. We find that the PT phase diagram exhibits an interesting dependence on the parameter α in such a way that in the softer limit up to a little above $\alpha=3$, the region of hexatic phase borders with liquid phase, at the same time reaching down to touch the gaseous phase. On the other hand, as the value of α increases, we find that the region of hexatic phase is shifted upward (in pressure), separated from the triple point, and no longer borders the gaseous phase.

II. SIMULATION RESULTS

In this work, we performed isobaric-isothermal (NPT) MD simulations using the modified Parrinello-Rahman (PR) method [35] combined with Nose-Hoover (NH) thermostat [36]. As for the mass of the particles, for convenience we set $m=1$, which implies that the time unit $t_0 \equiv \sqrt{m\sigma^2/\epsilon_0}$ also becomes unity. The equations of motion were integrated via the Nordsieck-Gear fifth-order predictor-corrector method with the integration time step of $\Delta t=0.002$. This guarantees the conservation of the total Hamiltonian without noticeable drift. In the simulations we used two empirical parameters, namely, the barostat mass $M_v=1$ and the thermostat mass $M_s=1$. Simulations with several other values ($M_v=0.1, 1, 10$, $M_s=0.1, 1, 10$) of the parameters were also performed with no essential change in the characteristic behavior.

A. The case of a soft- and long-ranged Morse potential: $\alpha=3$

Here, we first deal with the case of a soft- and long-ranged Morse potential with $\alpha=3.0$. Figure 2 shows the isothermal equation of state (at $T=0.2715$) on the pressure ver-

sus density plane. This was obtained by the NH MD simulations by decoupling the PR (isobaric) part from NH-PR MD equations of motions by taking $M_v=\infty$, which reduces to the isochoric-isothermal (NVT) condition. We define here the density ρ as $\rho \equiv N\sigma^2/V$, where N is the total number of particles and V is the total volume (area in two dimensions) of the system. Densities were chosen from the range $\rho=1.3-1.34$, with a density increment of $\Delta\rho=0.0025$, and the pressure was evaluated by means of the virial expression (with $k_B=1$). This range of the density corresponds to the region of transition from liquid to solid. For each density, $10^6-(3 \times 10^6)$ steps of integration were carried out for equilibration beginning with a configuration of triangular lattice, and, after equilibration, 10^7 steps of integration were collected for thermodynamic calculation.

The number of particles employed was $N=3600$. To reduce the finite-size boundary effect, we used a rhombic box (with the smaller side angle of 60°) for the shape of the system with periodic boundary conditions. However, independent results of ours from a square box did not show a significant difference (from those of rhombic box) with respect to the quantities of our interest.

Figure 2 shows that the isothermal curve increases monotonically near the transition region satisfying the condition of mechanical stability (unlike the discontinuity of density in a first-order transition) that the isothermal compressibility should be positive $K_T=(1/\rho)(\partial\rho/\partial P)_T > 0$. We may identify the boundary of stable hexatic phase as the values of the density where an abrupt change in the isothermal compressibility occurs. In this way, we estimate the density of solid-hexatic transition as $\rho_{s-h} \approx 1.3325$.

Although the change in isothermal compressibility is less conspicuous near the hexatic-liquid boundary, we see that, near the density $\rho \approx 1.31-1.315$, there exists a crossover in the isothermal compressibility. Below, we give an estimation of the density of hexatic-liquid transition by applying a theoretical expectation from KTHNY theory on the decay exponent of the spatial correlation of the orientational order parameter (see below).

The fact that the pressure within the hexatic phase is monotonically increasing as the density increases (with the resulting isothermal compressibility kept positive) appears to be very compelling evidence for a stable hexatic phase in thermal equilibrium. From the inset of Fig. 2 we can also see that, within the density interval for the hexatic phase, the rate of increase in the number of defects (which is defined as the number of sites of particles with five neighbors or seven neighbors), as the density is decreased, is larger than in the solid or liquid region, which is quite consistent with the behavior of the isotherm. High compressibility for the hexatic phase originates from the bulk modulus softened by a dramatic increase of the number of free dislocations from unbinding of the bound dislocation.

In previous studies on two-dimensional melting, a positive conclusion on the existence of a hexatic phase and continuous two-stage melting were often drawn from the simple features such as the absence of coexisting phases (i.e., homogeneous distribution of defects), direct observation of particle configurations, susceptibilities of orientational order, or the algebraic decay of spatial correlations of orientational order.

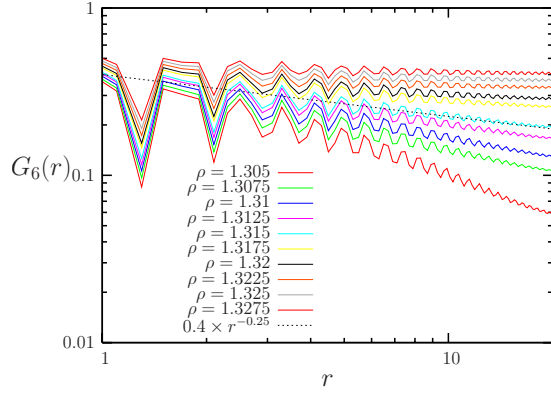


FIG. 3. (Color online) Spatial correlation functions (for $\alpha=3.0$) of the orientational order parameter for different densities at $T=0.2715$ corresponding to Fig. 2. The dashed line corresponds to the decay exponent of $\eta_6=1/4$.

However, in our independent study on Lennard-Jones systems [37], we observed that, although the system undergoes a first-order melting transition, the system exhibits features resembling those of a hexatic phase probably due to finite-size effects (even for the case of $N=40\,000$, which is the largest size we employed). These include homogeneous (single peak) distribution of orientational susceptibilities, and algebraic decay of the spatial correlations of the orientational order (at the same time with short-range translational order). In these cases, the alleged hexatic region is found to be actually located in the range of negative compressibility along a van der Waals-type curve, which implies a first-order transition. This probably originates from a finite-size effect resulting from a weakly first-order melting transition.

In contrast, in the present case of Morse systems, we find that both NPT and NVT ensemble simulations showed that there exists a region of stable hexatic phase.

In order to distinguish the orientational order of the phases, we have computed the orientational correlation function $G_6(r)$ defined as [2]

$$G_6(r) = \langle \psi_6(r) \psi_6^*(0) \rangle, \quad (2)$$

where the orientational order parameter is $\psi_6(r) = \frac{1}{N_i} \sum_j e^{6i\theta_{ij}(r)}$. Here, the sum on particle j is over the N_i neighbors of the particle i (corresponding to \vec{r} at the center) with θ_{ij} being the angle between the particles i and j with respect to a fixed reference axis. We regarded the particles within a cutoff radius as the neighbors, where the cutoff radius is chosen as the first minimum of the pair correlation function of the system. This method is found to be efficient and reliable for large-scale simulations.

Shown in Fig. 3 is the orientational correlation function for the range of the density ($1.3 \leq \rho \leq 1.34$). We find that, for the density range of $1.315 \leq \rho \leq 1.3325$, the correlation functions exhibit algebraic decays with the decay exponent $\eta < 1/4$, while for densities lower than these, they exhibit faster (exponential) decays in the long-time limit. At $\rho=1.315$, the exponent η_6 [defined by the condition $G_6(r) \sim r^{-\eta_6}$] is about $\eta_6=0.25$, corresponding to the limit of the power-law decay behavior in the KTHNY theory. This

range of the density is roughly consistent with the range of density mentioned above from the behavior of the isothermal compressibility.

Figure 4 shows snapshots of the particle configurations for four different densities near the hexatic phase region at temperature $T=0.2715$. We can see that there is a gradual increase of isolated dislocations as the density is decreased. For the case of $\rho=1.3275$ and 1.32 , for instance, we can identify isolated dislocations that indicate a characteristic feature of the hexatic phase. This is also consistent with the spatial correlation of the orientational order parameter as mentioned above (Fig. 3) displaying a regime with power-law decay in the orientational correlation function. We note that for these cases of hexatic phase, there exist along with the isolated dislocations some stringlike clusters of dislocations. At a lower density of $\rho=1.305$, we can see the emergence of isolated disclinations (lower left corner of the snapshot) in addition to proliferating local clusters of dislocations.

In order to further understand the nature of the hexatic phase, we obtained the histogram distribution [38] of the density order parameter for five system sizes ($N=400, 900, 1600, 3600$, and $10\,000$) under constant external pressure and temperature of $T=0.2715$ and $P=0.03$, where a hexatic phase is expected to occur from our measurement of the orientational correlations. In Fig. 5, we see that all the histograms exhibit single peaks. We also see that, as the number of particles increases, the peak height becomes larger with the width decreasing. This indicates that this region corresponds to a single phase region (unlike a solid-liquid mixture) consistent with the absence of a van der Waals loop in the pressure versus density curve.

Shown in the inset of Fig. 5 are the orientational correlation functions for the system sizes of $N=3600$ and $10\,000$ under the same conditions ($T=0.2715$ and $P=0.03$). We find that the correlation functions clearly exhibit algebraic decays with the decay exponent of $\eta_6 < 1/4$.

We can also investigate the dynamic characteristics of the system in the hexatic phase in terms of the time dependence of the orientational order parameter. One example is shown in Fig. 6 for $T=0.2715$ and $P=0.03$, which belongs to the hexatic phase region. Here for convenience we presented only the absolute modulus $|M_6|$ of the global orientational order parameter M_6 defined as

$$M_6 \equiv \frac{1}{N} \sum_r \psi_6(r). \quad (3)$$

We find that the global orientational order parameter exhibits a considerable fluctuation in time around $|M_6| \sim 0.5$, which, even though the magnitude is clearly smaller than that of a solid phase (for which, typically, $|M_6| \geq 0.7$), is still a non-negligible magnitude (for the present case of a finite-size system) that is quite unlike the case of a liquid phase (where $|M_6| \leq 0.2$). This kind of strong fluctuation of the order parameter can be considered as one of the characteristic features of critical states such as the hexatic phase. Indeed, we found that the power spectrum of the time dependence of the order parameter exhibits a power-law behavior characteriz-

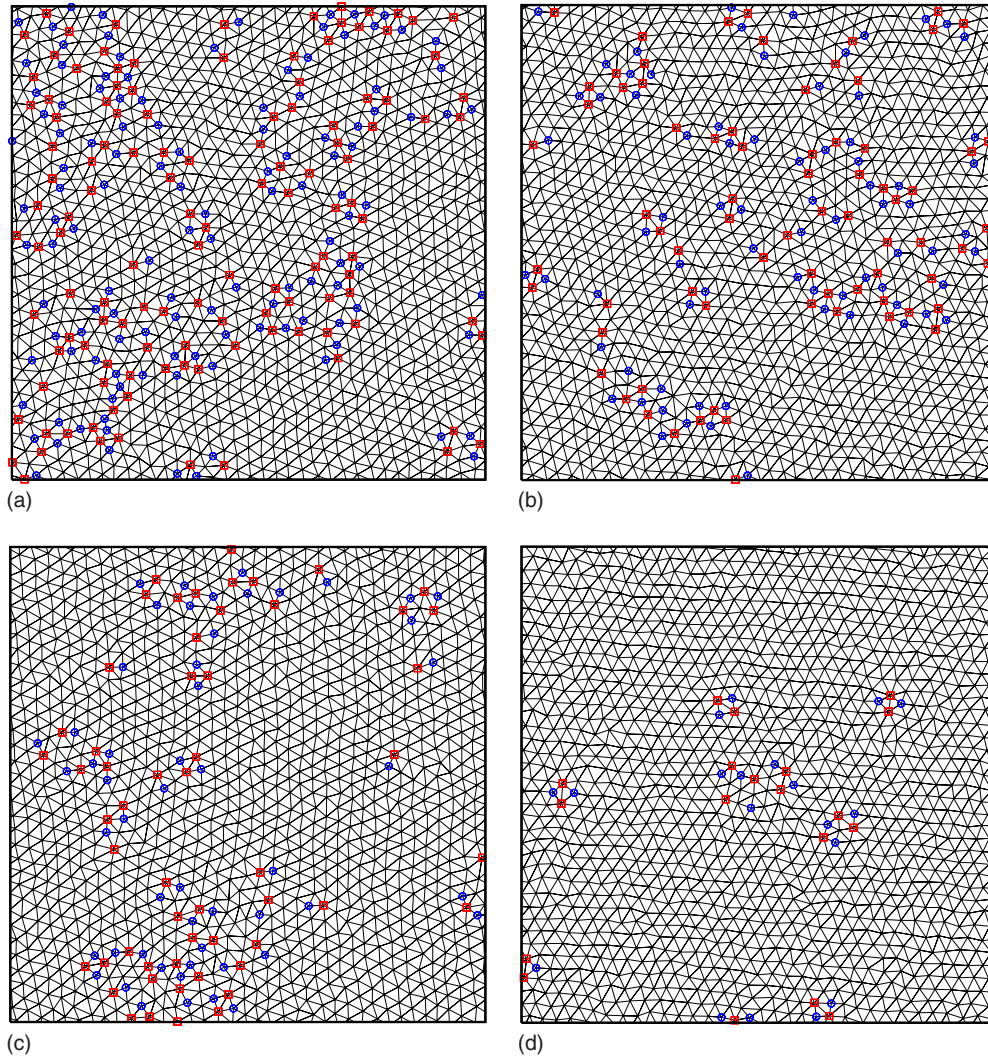


FIG. 4. (Color online) Configurations (for $\alpha=3.0$) at $T=0.2715$ for densities (a) $\rho=1.305$, (b) 1.32, (c) 1.3275, and (d) 1.34. Symbols of blue open circles and red open squares denote the defect sites of particles with five nearest neighbors and seven nearest neighbors, respectively.

ing a critical state. Details on these dynamic characteristics will be presented elsewhere [37].

By tracing the $P-\rho$ equation of state and calculating the spatial correlation of the orientational order parameter for this system, a qualitative PT phase diagram for $\alpha=3.0$ has been obtained, which is shown in Fig. 7. This corresponds to one of the possible phase diagrams suggested by Nelson [39]. To determine the approximate shape of the hexatic region, we used some points on the hexatic-liquid phase boundary obtained from approximate calculations including $(T_h, P_h) = (0.2715, 0.01)$, $(0.4, 5.175)$, and $(0.6, 24.31)$.

We also obtained isothermal curves at higher temperatures of $T=0.8, 0.85$, and 1. At $T=0.8$, a van der Waals loop (for gas-liquid coexistence) was found. And at $T=1.0$, the curve increased monotonically, indicating that this temperature is above the critical temperature. Since, on the isotherm at $T=0.85$, the inflection point is shown approximately at $P=0.95$, we can estimate the critical point as $T_c \approx 0.85$ and $P_c \approx 0.95$.

An important feature of the phase diagram for the present system of $\alpha=3.0$ is that the region of hexatic phase extends

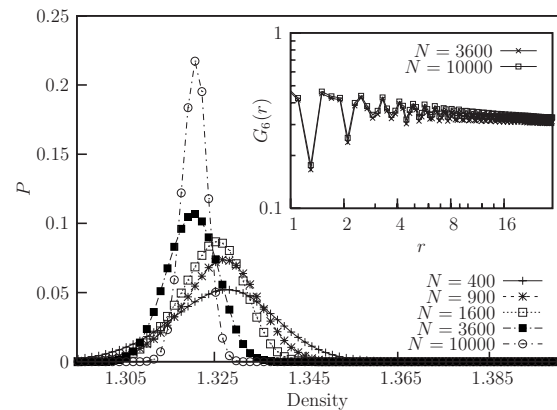


FIG. 5. Histogram distributions (for $\alpha=3.0$) of the density in isobaric-isothermal ensemble simulations at $P=0.03$, $T=0.2715$ for system sizes $N=400, 1600, 3600$, and 10 000, respectively. The inset shows the spatial correlation of the orientational order parameter for system sizes $N=3600$ and 10 000. In both the inset and the main figure the lines are only guides for the eyes.

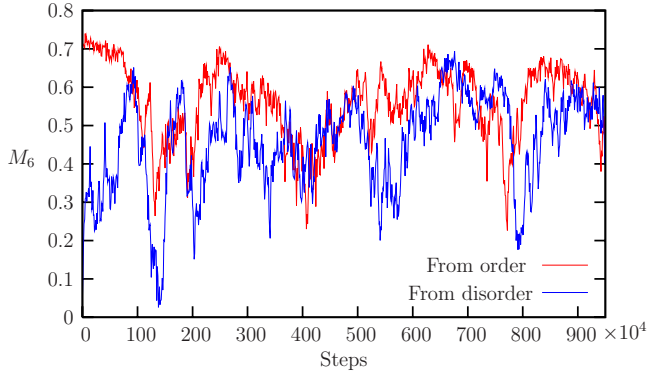


FIG. 6. (Color online) Evolution of the orientational order parameter M_6 corresponding to $N=1600$ system (with $\alpha=3.0$) in Fig. 4 at $P=0.03$, $T=0.2715$. We can see strong fluctuations of the orientational order parameter which is expected in a critical hexatic phase.

down to the solid-gas sublimation line at low pressures. That is to say, the hexatic phase touches the area near the conventional triple-point region. At these low pressures, the hexatic phase would melt directly into a gaseous phase via a first-order transition.

From our simulations, we observe a hexatic phase in coexistence with a gaseous phase at low temperatures. Along isotherms at low temperatures, with decreasing density, the solid goes into the hexatic phase, and then at further decrease of the density, the hexatic phase goes into coexistence with the gaseous phase. This is illustrated in Fig. 8, where the hexatic phase coexists with gas at temperature $T=0.27$. From our calculations, we estimate that the temperature T_{s-h-g} of the triple coexistence between the solid, hexatic, and gas phases is located in the region $0.25 < T_{s-h-g} < 0.27$.

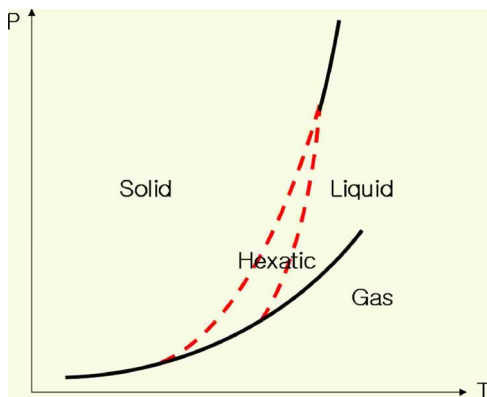


FIG. 7. (Color online) A schematic phase diagram for the Morse system with $\alpha=3.0$. Solid lines denote first-order transitions and dashed lines second-order ones. At very high pressures and temperatures, the behavior of the system is dominated by the hard core of the potential. Therefore, as in the case of nonattractive potentials, systems at arbitrarily high pressure may undergo a first-order transition. The present diagram presumes the existence of an upper bound for the hexatic region in the PT diagram. Note that the hexatic-liquid transition line increases monotonically with positive slope in the P - T plane. It was also shown from simulations that the hexatic phase is extended above (in the value of the pressure) the critical point ($T_c \approx 0.85$, $P_c \approx 0.95$).

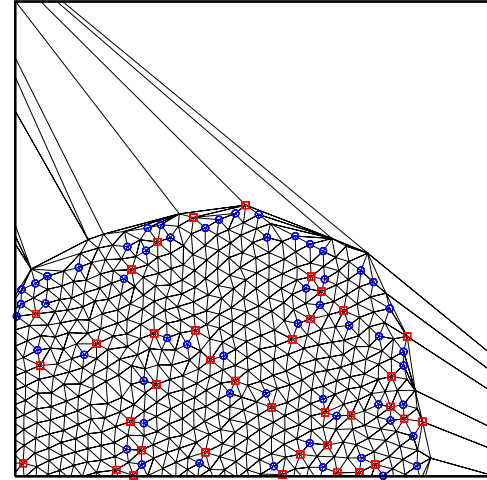


FIG. 8. (Color online) Configuration of the system with $\alpha=3.0$ (Delaunay triangulation from Voronoi construction) at $T=0.27$ and density $\rho=0.4$, showing coexistence of hexatic and gaseous phases. Voronoi lines outside the cluster are connected with particles belonging to other clusters. Symbols of blue open circles and red open squares denote the defect sites of particles with five nearest neighbors and seven nearest neighbors, respectively.

Figure 9(a) shows part of an isotherm that goes through the hexatic phase and the gas phase with the inset displaying the extended part of the curve. Note that the pressure crosses zero in the density region of $1.32 < \rho < 1.3225$. In order to understand how the system develops along the isothermal curve under expansion (i.e., decreasing density), we calculated, for densities near the hexatic-gas transition, the time dependence of the magnitude of the global orientational order parameter M_6 defined above in Eq. (3) and also that of the translational order parameter M_T defined as

$$M_T \equiv \frac{1}{N} \sum_r \rho_G(r) \quad (4)$$

$$\equiv \frac{1}{N} \sum_r \exp(i\vec{G} \cdot \vec{r}). \quad (5)$$

Here, \vec{G} is a reciprocal-lattice vector and \vec{r} refers to the positions of particles. As for finding the appropriate direction for the \vec{G} vector, we followed the method devised by Bagchi *et al.* [40].

As can be seen from Figs. 9(b) and 9(c), the system (at $T=0.27$) remains in a hexatic phase for all of the four densities including the negative pressure region with quasi-long-range orientational order but with no translational order. This corresponds to the region of an extended metastable hexatic phase analogous to a conventional metastable solid or liquid.

Figure 9(a) shows the corresponding isotherm ($T=0.27$) where we see that the hexatic phase extends from pressure 0.041 at density 1.33 down to the negative pressure region. Even though it is rather difficult to identify the value of the pressure for the exact hexatic-to-gas transition, we know at least that, for thermal equilibrium, gas should be at a positive pressure. There is also an upper bound for the pressure for

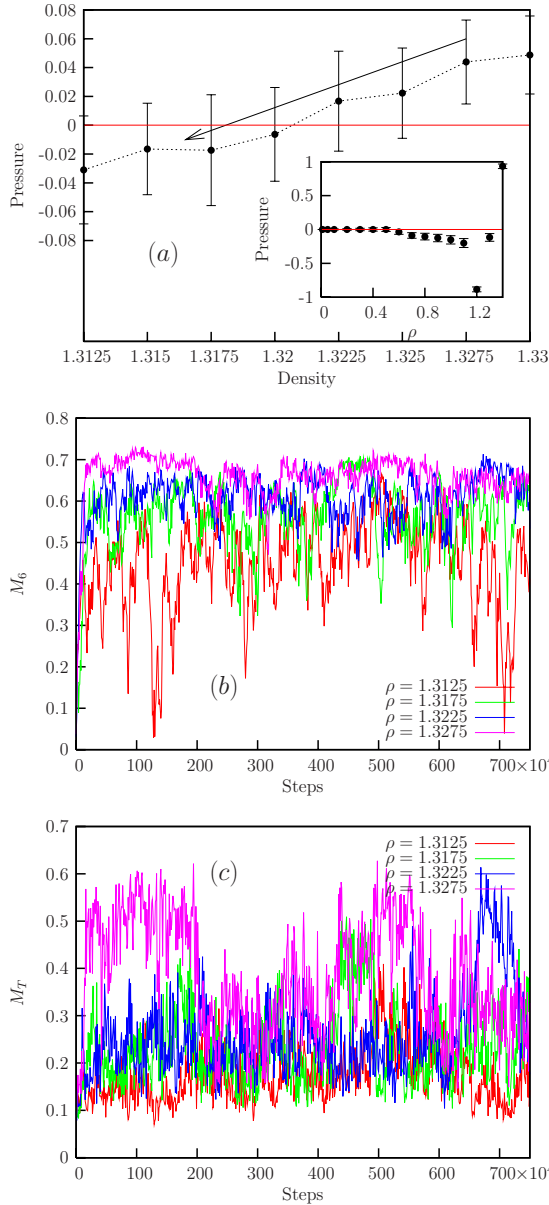


FIG. 9. (Color online) (a) Isothermal curve at $T=0.27$ with $\alpha=3.0$. The inset shows the extended line down to lower density regime and the arrow indicates crossover from hexatic phase to metastable one. (b) Time dependence (for $\alpha=3.0$) of the orientational order parameter for different densities at $T=0.27$. (c) Time dependence (for $\alpha=3.0$) of the translational order parameter for different densities at $T=0.27$.

the transition which is the pressure for the solid-gas spinodal point (below $P=10^{-3}$). This means that a hexatic phase will also intervene between the solid and gas at a positive pressure in the phase diagram. This hexatic phase will turn into a gaseous state via a first-order hexatic-gas transition.

Applying this idea to the isothermal curve at $T=0.25$ [Fig. 10(a)] and the time dependence of the orientational and translational order parameter in Figs. 10(b) and 10(c), we also found that the solid phase (which has long-range orientational and quasi-long-range translational order) is extended to negative pressures implying solid-gas coexistence. Therefore, we can see that the lowest temperature for the occur-

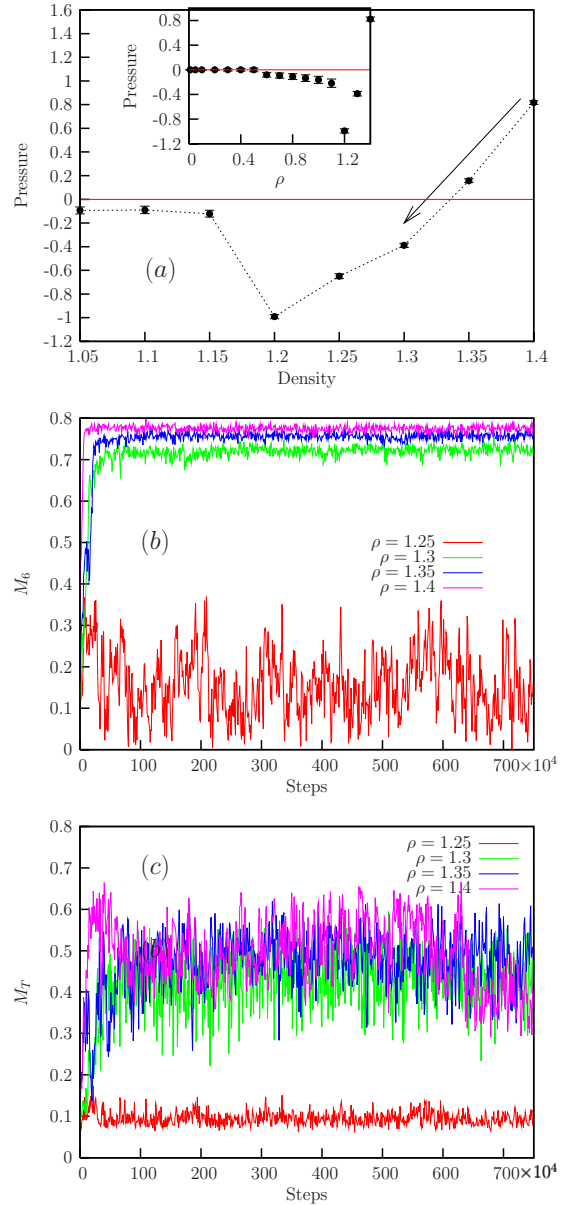


FIG. 10. (Color online) (a) Isothermal curve (for $\alpha=3.0$) at $T=0.25$. The inset shows the extended line down to very low density and the arrow indicates crossover from solid to metastable solid. (b) Time dependence (for $\alpha=3.0$) of the orientational order parameter for different densities at $T=0.25$. (c) Time dependence (for $\alpha=3.0$) of the translational order parameter for different densities at $T=0.25$.

rence of a hexatic phase is located between $T=0.25$ and 0.27 .

In the PT plane, this means that, at low pressures (but larger than some small positive pressure), with increasing temperature, a solid goes into a hexatic phase and then into a gaseous phase via a first-order transition that will preempt the continuous unbinding of disclination pairs. Since the unbinding of bound disclination pairs cannot take place with an abrupt jump of volume into gas, some kind of nucleation process must intervene in the hexatic-gas transition, which will result in a first-order transition.

We have also investigated the cases of soft Morse potential with a smaller value of the parameter $\alpha=2.5$. For the

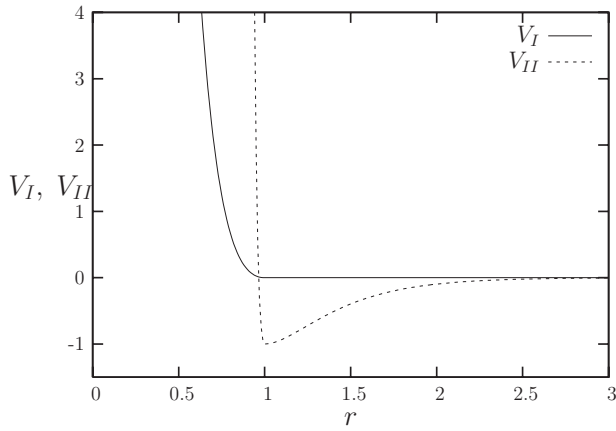


FIG. 11. Modified potentials V_I (solid line) and V_{II} (dotted line). V_I is obtained from the Morse potential with $\alpha=3.0$ by removing the attractive part (replaced by a flat potential) and shifting the repulsive part upward to match the flat potential smoothly. On the other hand, V_{II} is obtained from the Morse potential with $\alpha=3.0$ by replacing the repulsive part by an almost hard-core repulsive wall corresponding to $\alpha=20.0$ while leaving the attractive part intact.

case of $\alpha=2.5$ (at $T=0.2715$), which corresponds to an even softer potential than the case of $\alpha=3.0$ considered above, we found that the behavior of the system in terms of the hexatic phase formation is similar to the case of $\alpha=3.0$, with the only quantitative difference being the existence of a wider region of hexatic phases than the case of $\alpha=3.0$.

B. Modifications of the Morse potential and melting

Now, in order to understand the effect of the shape of the potential in determining the tendencies of hexatic phase formation, we first modified the Morse potential with $\alpha=3.0$ such that the attractive tail part is removed and replaced by a flat potential (which is shown in Fig. 11 as a solid line denoted by V_I). In this case, we could not observe a stable hexatic phase at the typical temperatures where hexatic phases were found when an attractive part of the potential was present. This is evidenced by the existence of a van der Waals loop in the equation of state (Fig. 12) and also by the histogram of the density order parameter. In particular, the histogram distribution [38] of the density order parameter for different system sizes ($N=900, 1600$, and 3600) under external constant pressure (NPT) with $T=0.2715$ and $P=4.85$, which is shown in the inset of Fig. 12, exhibits double peaks. We can see that the ratio between the peak height and the valley for $N=3600$ becomes larger than that for $N=900$, which corresponds to typical characteristics (the growth of the free-energy barrier) of first-order transitions with increasing system size.

In another modification of the potential, we replaced the repulsive-core part of the Morse potential with $\alpha=3$ by an almost hard-core potential corresponding to the Morse potential with $\alpha=20$. We note that the attractive part is kept the same as the original $\alpha=3$ case (shown as a dotted line in Fig. 11 denoted by V_{II}). For this case also, we found that the system shows transitions of a first-order nature (numerical results are not shown here). These results imply that the soft-

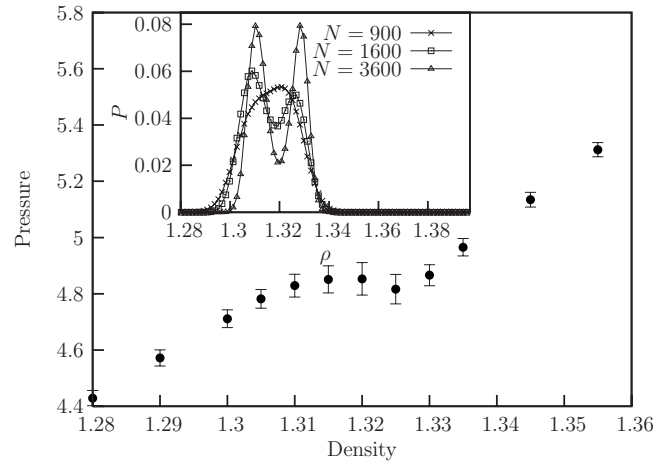


FIG. 12. Pressure vs density at the temperature $T=0.2715$ and $P=4.85$ obtained from NPT ensemble with $N=3600$ particles for the repulsive Morse potential (derived from $\alpha=3.0$). The inset shows the histogram of the density order parameter. We find a van der Waals loop in the pressure-density relation as well as the double peaks in the histogram of density order parameter (the inset) indicating a first-order nature of the melting in this system of repulsive potential.

ness of both the repulsive and the attractive part is important for the existence of the hexatic phase.

C. The cases of Morse potentials with larger values of α : $\alpha=3.5, 4.0$

Now, when the parameter α gets larger, we may expect that the formation of hexatic phases will be hindered due to the increasing hard-core repulsion and the shorter range of the attractive part of the potential. This may result in distinct characteristics in terms of the hexatic phase formation.

Indeed, when the system with $\alpha=3.5$ was investigated, we could find a qualitative difference in the characteristics of the hexatic phase region where the region of the hexatic phase in the PT plane is disconnected from the triple point and is no longer bordering on the region of the gaseous phase. The inset of Fig. 13 exhibits a van der Waals-like isotherm at $T=0.5$ (above the triple point), which implies a first-order transition. This kind of first-order nature has also been shown at $T=0.35$ ($P \approx 0.75$). Interestingly, at higher temperature of $T=0.7$, it changes to a second-order phase transition as shown in Fig. 13 with similar behavior of a second-order nature being extended to higher temperatures such as $T=1.0$ (with the pressure P_m of solid-hexatic transition $P_m \approx 34.7$ and the pressure P_i of hexatic-liquid transition $P_i \approx 34.27$).

Therefore, we can see here that, as the value of α gets larger, the onset of the hexatic phase in the PT phase diagram gets shifted upward in pressure and temperature. In order to further confirm this expectation, we investigated the case of $\alpha=4.0$. While at $T=0.7$ the system undergoes a first-order transition (with the pressure at melting $P_m \approx 7.85$), at $T=1.0$ (which is above the critical point) it exhibits a second-order transition (with $P_m \approx 18.4$ and $P_i \approx 18.1$) implying that the onset of a hexatic phase is shifted further upward, which

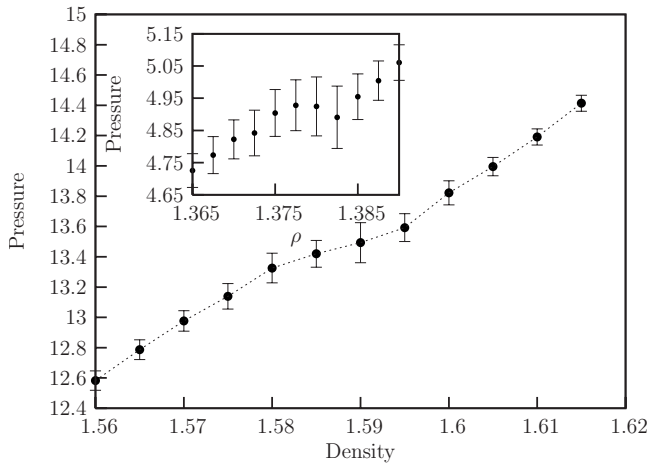


FIG. 13. Isothermal curve for the case of $\alpha=3.5$ at $T=0.7$ and 0.5 (the inset).

is consistent with our expectation. From these features of the hexatic region, we may depict the schematic phase diagrams for the case of $\alpha=3.5$ as shown in Fig. 14. To identify the location of the critical point, isothermal curves over $\rho=0.1-1.0$ at $T=0.6, 0.7, 0.8$, and 0.9 were calculated. Whereas it exhibits a van der Waals curve (going through a liquid-gas phase) at $T=0.6, 0.7$, a monotonic increase is seen for temperatures above $T=0.7$, so that a critical line can be located between $T=0.7$ and 0.8 . Thus, the location of the onset of the hexatic phase is located below the critical point.

In the case of the system with $\alpha=3.5$, we may ask why the hexatic phase exists at relatively higher pressures whereas it disappears at lower pressures. This may be explained in the framework discussed in Secs. I and II. Namely, near melting, a system under higher pressures would behave in a way similar to another system with smaller values of α (in terms of the repulsive part, to be more precise). An increase of pressure may be considered as a relative increase of the range of the potential. Of course, this argument would apply only when the repulsive core is soft enough for the system to respond easily to external pressures.

III. SUMMARY AND DISCUSSIONS

We have shown in this work that the softness of the repulsive part as well as the longer range of the attractive part of the interaction are important for the existence of a stable hexatic phase in simple atomic systems. This was supported by modification of the Morse potential (with $\alpha=3.0$) replacing the attractive tail by a flat potential and retaining only the repulsive part of the interatomic potential of the system, and also by another modification where the repulsive part was replaced by a very steep potential with the attractive part kept unchanged.

These properties can also explain the existence of a hexatic phase at higher pressures in which, due to the decrease of the interparticle distance, the particles of the system may be considered as experiencing interparticle potential with an effectively wider range. Due to this generic nature of the hexatic phase, the hexatic regime in the phase diagram of

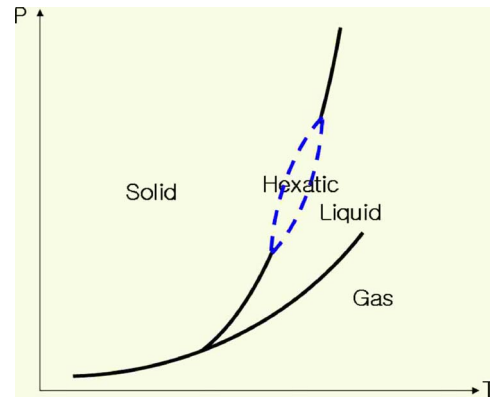


FIG. 14. (Color online) A schematic phase diagram for the Morse system with $\alpha=3.5$. We can see that the hexatic phase region does not touch on the triple point. Solid curves denote first-order transitions and the dashed lines second-order transitions. The location of the onset of hexatic phase is located below the critical point.

pressure versus temperature shrinks as the range of the potential decreases, and also the lower bound of the hexatic phase is shifted into higher pressures and temperatures. This nature also implies the existence of an upper bound (in pressure and temperature) for the hexatic regime since, at much higher pressures and temperatures, the attractive part of the interatomic potential plays a negligible role, with the behavior of the system being determined by a stiff repulsive core.

For longer-ranged potentials with smaller values of α such as $\alpha=3.0, 2.5$, the hexatic region in the PT phase diagram borders on both a liquid as well as a gas phase. At low pressures, as the temperature is increased, the solid goes into the hexatic phase and then the hexatic phase turns into a gaseous phase via a first-order transition. At higher pressures, the solid goes into the hexatic phase and then into liquids via a standard KTHNY scenario of continuous unbinding of dislocations and disclinations. As the potential gets stiffer and short ranged (larger values of α such as $\alpha=3.5, 4.0$), it was found that the region of hexatic phase gets reduced and the hexatic phase regime does not border the gaseous phase (thus not touching the triple-point region).

It would be interesting to find a more microscopic mechanism behind this behavior of the hexatic phase formation depending on the range of the attractive potential and the softness of the repulsive core. Presumably, these potentials characterized by a soft and wide bottom region give rise to strong local structural correlation of the particles that will act favorably for the formation of the hexatic phase. In relation to this, it may be worth mentioning the works of Wales *et al.* reporting that decreasing the range of the interatomic potential decreases cooperativity of the atoms in the system because the motion of an atom depends only on its local environment of closest atoms [41]. The fact that a longer range of potential is preferred for the existence of the hexatic phase is, therefore, correlated probably to the local cooperativity of atoms. These may also be realizable in the cases of systems described by long-range repulsive potentials [42]. A similar scenario was suggested by Sear and Frenkel (see Ref. [43]).

- [1] D. R. Nelson, *Defects and Geometry in Condensed Matter Physics* (Cambridge University Press, Cambridge, 2002).
- [2] B. I. Halperin and D. R. Nelson, Phys. Rev. Lett. **41**, 121 (1978).
- [3] D. R. Nelson and B. I. Halperin, Phys. Rev. B **19**, 2457 (1979).
- [4] A. P. Young, Phys. Rev. B **19**, 1855 (1979).
- [5] J. M. Kosterlitz and D. J. Thouless, J. Phys. C **6**, 1181 (1973).
- [6] K. J. Strandburg, Rev. Mod. Phys. **60**, 161 (1988).
- [7] C. A. Murray and D. H. Van Winkle, Phys. Rev. Lett. **58**, 1200 (1987).
- [8] R. E. Kusner, J. A. Mann, J. Kerins, and A. J. Dahm, Phys. Rev. Lett. **73**, 3113 (1994).
- [9] A. H. Marcus and Stuart A. Rice, Phys. Rev. Lett. **77**, 2577 (1996).
- [10] K. Zahn, R. Lenke, and G. Maret, Phys. Rev. Lett. **82**, 2721 (1999).
- [11] R. Pindak, D. E. Moncton, S. C. Davey, and J. W. Goodby, Phys. Rev. Lett. **46**, 1135 (1981).
- [12] J. D. Brock, A. Aharony, R. J. Birgeneau, K. W. Evans-Lutterodt, J. D. Litster, P. M. Horn, G. B. Stephenson, and A. R. Tajbakhsh, Phys. Rev. Lett. **57**, 98 (1986).
- [13] M. Cheng, J. T. Ho, S. W. Hui, and R. Pindak, Phys. Rev. Lett. **61**, 550 (1988).
- [14] C.-F. Chou, A. J. Jin, S. W. Hui, C. C. Huang, and J. T. Ho, Science **280**, 1424 (1998).
- [15] D. E. Angelescu, C. K. Harrison, M. L. Trawick, R. A. Register, and P. M. Chaikin, Phys. Rev. Lett. **95**, 025702 (2005).
- [16] J. S. Olafsen and J. S. Urbach, Phys. Rev. Lett. **95**, 098002 (2005).
- [17] P. M. Reis, R. A. Ingale, and M. D. Shattuck, Phys. Rev. Lett. **96**, 258001 (2006).
- [18] For earlier works, see Ref. [6] and references therein.
- [19] S. T. Chui, Phys. Rev. Lett. **48**, 933 (1982).
- [20] S. T. Chui, Phys. Rev. B **28**, 178 (1983).
- [21] B. Joos and M. S. Duesbery, Phys. Rev. Lett. **55**, 1997 (1985).
- [22] B. Joos and M. S. Duesbery, Phys. Rev. B **33**, 8632 (1986).
- [23] Y. Saito, Phys. Rev. Lett. **48**, 1114 (1982).
- [24] J. D. K. Doye and D. J. Wales, Science **271**, 484 (1996).
- [25] P. Shah and C. Chakravarty, Phys. Rev. Lett. **88**, 255501 (2002).
- [26] K. J. Strandburg, J. A. Zollweg, and G. V. Chester, Phys. Rev. B **30**, 2755 (1984).
- [27] J. Lee and K. J. Strandburg, Phys. Rev. B **46**, 11190 (1992).
- [28] M. A. Bates and D. Frenkel, Phys. Rev. E **61**, 5223 (2000).
- [29] C. H. Mak, Phys. Rev. E **73**, 065104(R) (2006).
- [30] K. Chen, T. Kaplan, and M. Mostoller, Phys. Rev. Lett. **74**, 4019 (1995).
- [31] F. L. Somer, G. S. Canright, T. Kaplan, K. Chen, and M. Mostoller, Phys. Rev. Lett. **79**, 3431 (1997).
- [32] F. L. Somer, Jr., G. S. Canright, and T. Kaplan, Phys. Rev. E **58**, 5748 (1998).
- [33] P. Bladon and D. Frenkel, Phys. Rev. Lett. **74**, 2519 (1995).
- [34] T. Chou and D. R. Nelson, Phys. Rev. E **53**, 2560 (1996).
- [35] M. Li and W. L. Johnson, Phys. Rev. B **46**, 5237 (1992).
- [36] S. Nose, J. Chem. Phys. **81**, 511 (1984).
- [37] Sang Il Lee and Sung Jong Lee (unpublished).
- [38] J. Lee and J. M. Kosterlitz, Phys. Rev. Lett. **65**, 137 (1990).
- [39] See p. 80 of Ref. [1].
- [40] K. Bagchi, H. C. Andersen, and W. Swope, Phys. Rev. Lett. **76**, 255 (1996).
- [41] D. J. Wales, J. Chem. Phys. **101**, 3750 (1994).
- [42] H. H. von Grünberg, P. Keim, and G. Maret, in *Soft Matter* (WILEY-VCH Verlag, Berlin, 2007), Vol. 3, Chap. 2.
- [43] Richard P. Sear and Daan Frenkel, Phys. Rev. Lett. **90**, 195701 (2003).